Metalloporphyrin Mixed-Valence π-Cation Radicals: Solution Stability and Properties

Kristin E. Brancato-Buentello, Seong-Joo Kang, and W. Robert Scheidt*

Contribution from the Department of Chemistry and Biochemistry, University of Notre Dame, Notre Dame, Indiana 46556

Received May 20, 1996[⊗]

Abstract: Solution equilibria and optical spectra of several metallooctaethylporphyrin π-cation radicals have been examined in methylene chloride solution. The several π-cation radical species, $[M(OEP^{\bullet})]Y$ (M = Cu, Ni, Zn, Pd, or VO; Y = ClO_4^- or $SbCl_6^-$), are found to dimerize to form $[M(OEP^{\bullet})]_2^{2+}$. These dimeric species are characterized by the appearance of a new, strongly concentration-dependent near-infrared absorption band. This band is found in the region of 900−960 nm for all compounds except for the vanadyl complex which absorbs farther to the red at 1375 nm. The equilibrium constants for the dimerization reaction ($2[M(OEP^{\bullet})]^+$ (K_D) $[M(OEP^{\bullet})]_2^{2+}$) have been evaluated from multiple-wavelength, concentration-dependent absorption data. Equimolar solutions of these π-cation radicals and their analogous neutral M(OEP) derivatives react to form new binuclear species, $[M(OEP^{\bullet/2})]_2^+$, in which the single radical electron is delocalized over both porphyrin rings. These new species, for which we suggest the term "mixed-valence" π-cation radical and which bear a formal relationship to the oxidized special pair of photosynthetic reaction centers, also display a near-infrared absorption band. The near-IR band is however distinctly different from that of the π-cation radical dimers. Equilibrium constants for the formation of these new species ($M(OEP) + [M(OEP^{\bullet})]^+$ (K_{MV}) $[M(OEP^{\bullet/2})]_2^+$), have also been determined. The values of K_{MV} are 10−100-fold larger than the analogous dimerization constant K_D. Values of ΔH and ΔS have been obtained for both equilibrium processes. The variations in K_{MV} and K_D values are largely the consequence of entropy differences that probably result from a much stronger solvation of the π-cation radical compared to the neutral porphyrin.

Introduction

Electronic interactions between the π systems of two or more porphyrin molecules in close proximity are believed to be important in defining the properties of the supramolecular ensemble. Notable examples of such interacting porphyrin π systems are those found in photosynthetic proteins[1] and in linearly stacked arrays that are organic conductors.[2] The photosynthetic proteins include the light-harvesting chlorophyll arrays[3] and the photosynthetic reaction center (RC)[4] special pairs.[5] The photoinduced formation of the one-electron oxidized reaction center special pair (the primary donor, often called P^+) is the first step in the conversion of light energy to chemical energy. The presence of a strongly interacting pair of bacteriochlorophylls in photosynthetic bacterial reaction centers was originally inferred from spectroscopic measurements.[6] In the green plant photosynthetic apparatus, a similar, although apparently less strongly interacting, pair of chlorophyll *a* molecules is the primary donor for at least one of the photosystem reaction centers (PS II).[7,8]

X-ray crystal structures of bacterial photosynthetic reaction centers from several organisms[9−12] have now provided detailed information about the ground state geometry of the special pair, P. The special pair has a cofacial arrangement of the two bacteriochlorophyll rings with effective overlap of one pyrrole ring from each macrocycle. The overlap of porphyrin rings has been frequently observed in the solid-state structures of porphyrin compounds.[13] However, most porphyrin compounds exhibit stronger intermolecular interactions than that displayed by the photosynthetic special pairs as judged by the geometric criterion of the degree of inter-ring overlap. The apparent importance of the cofacial bacteriochlorophyll dimer in defining the photophysics and photoinduced electron transfer of the entire RC system, e.g., the excited state P* to oxidized P^+ transition, has led to the synthesis and characterization of a number of bisporphyrin derivatives. Two different, broad classes of

[⊗] Abstract published in *Advance ACS Abstracts,* March 1, 1997.

(1) (a) Gregory, R. P. F. *Photosynthesis*; Chapman and Hall: New York, 1989. (b) *Photosynthesis*; Amesz, J., Ed.; Elsevier: New York, 1987.

(2) Hoffman, B. M.; Ibers, J. A. *Acc. Chem. Res.* **1983**, *16*, 15.

(3) (a) Kühlbrandt, W.; Wang, D. N.; Fujiyoshi, Y. *Nature (London)* **1994**, *367*, 614. (b) McDermott, G.; Prince, S. M.; Freer, A. A.; Hawthornthwaite-Lawless, A. M.; Papiz, M. Z.; Cogdell, R. J.; Isaacs, N. W. *Nature (London)* **1995**, *374*, 517.

(4) Abbreviations used in this paper include the following: RC, photosynthetic reaction center; PS, photosystem; P, the bacteriochlorophyll special pair; OEP, octaethylporphyrin; $OEP^{\bullet}$, octaethylporphyrin π-cation radical; $OEP^{\bullet/2}$, octaethylporphyrin mixed-valence π-cation radical.

(5) *The Photosynthetic Reaction Center*; Deisenhofer, J., Norris, J. R., Eds.; Academic Press: New York, 1993; Vol. 2.

(6) (a) McElroy, J. D.; Feher, G.; Mauzerall, D. C. *Biochim. Biophys. Acta* **1969**, *172*, 180. (b) Norris, J. R.; Uphaus, R. A.; Crespi, H. L.; Katz, J. J. *Proc. Natl. Acad. Sci. U.S.A.* **1971**, *68*, 625. (c) Norris, J. R.; Scheer, H.; Katz, J. J. *Ann. N. Y. Acad. Sci.* **1975**, *244*, 260. (d) Feher, G.; Hoff, A. J.; Isaacson, R. A.; Ackerson, L. C. *Ann. N. Y. Acad. Sci.* **1975**, *244*, 239. (e) Davis, M. S.; Forman, A.; Hanson, L. K.; Thornber, J. P.; Fajer, J. *J. Phys. Chem.* **1979**, *83*, 3325.

(7) (a) Nanba, O.; Satoh, K. *Proc. Natl. Acad. Sci. U.S.A.* **1987**, *84*, 109. (b) Michel, H.; Deisenhofer, J. *Biochemistry* **1988**, *27*, 1. (c) Lösche, M.; Satoh, K. *Biophys. J.* **1988**, *53*, 270a. (d) van Mieghem, F. J. E.; Satoh, K.; Rutherford, A. W. *Biochim. Biophys. Acta* **1991**, *1058*, 379.

(8) An alternate view concerning dimers in PS II has been recently forwarded: Durrant, J. R.; Klug, D. R.; Kwa, S. L. S.; van Grondelle, R.; Porter, G.; Dekker, J. P. *Proc. Natl. Acad. Sci. U.S.A.* **1995**, *92*, 4798.

(9) (a) Deisenhofer, J.; Epp, O.; Miki, K.; Huber, R.; Michel, H. *J. Mol. Biol.* **1984**, *180*, 385. (b) Deisenhofer, J.; Epp, O.; Miki, K.; Huber, R.; Michel, H. *Nature* **1985**, *318*, 618.

(10) Deisenhofer, J.; Epp, O.; Sinning, I.; Michel, H. *J. Mol. Biol.* **1995**, *246*, 429.

(11) (a) Allen, J. P.; Feher, G.; Yeates, T. O.; Komiya, H.; Rees, D. C. *Proc. Natl. Acad. Sci. U.S.A.* **1987**, *84*, 5730. (b) Chirona, A. J.; Lous, E. J.; Huber, M.; Allen, J. P.; Schenck, C.; Paddock, M. L.; Feher, G.; Rees, D. C. *Biochemistry* **1994**, *33*, 4584.

(12) El-Kabbani, O.; Chang, C.-H.; Tiede, D.; Norris, J.; Schiffer, M. *Biochemistry* **1991**, *30*, 5361.

(13) Scheidt, W. R.; Lee, Y. J. Recent Advances in the Stereochemistry of Metallotetrapyrroles. *Struct. Bonding (Berlin)* **1987**, *64*, 1.

S0002-7863(96)01695-2 CCC: $14.00

bisporphyrin compounds have been studied as RC models: covalently linked porphyrin dimers and larger assemblies[14] and lanthanide and actinide bisporphyrin or "double-decker" derivatives.[15] These two systems can in principle be used to form oxidized (π-cation radical) species with oxidation states that are formally analogous to P^+, and oxidized double-deckers, in particular, have been studied to develop a further understanding of the electronic structure of P^+. The double-decker compounds have been particularly attractive for study as RC models because of their necessarily cofacial structures and the possibility of varying the porphyrin interplanar spacing by changing the central metal ion. However, the completely overlapped, cofacial geometry of these double-deckers is distinctly different from the slipped conformation of the special pair observed in the reaction center structures. The geometric connection constraint(s) in the covalently linked bisporphyrins also leads to structures different than that displayed by the special pair. Nonetheless, oxidation of covalently linked bisporphyrins does suggest that the geometry between the two porphyrin rings is important in yielding derivatives with physicochemical properties similar to those of photooxidized RC special pairs.

Recently,[16] we have shown that some metallooctaethylporphyrinate derivatives can be oxidized to form π-cation radical derivatives in which only one electron is removed per two porphyrin rings rather than the expected one electron per porphyrin ring. Thus these new dimeric, supramolecular assemblies of general formula $[M(OEP^{\bullet/2})]_2^+$ have the same formal oxidation level as the photooxidized special pair of reaction centers. We suggest "mixed-valence π-cation radical" as a descriptive name for this new class of synthetic porphyrin derivatives. The apparent stability of the mixed-valence π-cation radicals, particularly the absence of significant disproportionation in solution, was surprising. Systems of $[M(OEP^{\bullet/2})]_2^+$ that have been studied include derivatives where M = Cu, Ni, Zn, Pd, or VO. A limited set of heterodimeric systems have also been investigated. In this paper, we examine the solution properties of these mixed-valence π-cation radical species including their UV/vis/near-IR spectral properties. Their spectral properties are distinctly different from those of the related neutral or classical π-cation radical metalloporphyrin species; the differences are most pronounced in the near-IR region. We also report the formation constants for $[M(OEP^{\bullet/2})]_2^+$ and the π-cation radical dimers, $[M(OEP^{\bullet})]_2^{2+}$, in methylene chloride solution. Values of ΔH and ΔS are reported for both equilibrium processes. We have reported the detailed solid-state structures of three crystalline $[M(OEP^{\bullet/2})]_2^+$ species elsewhere.[17] The combination of solid-state structural and solution studies reported herein makes it evident that the mixed-valence π-cation radicals have many properties that are distinct from those of either neutral or π-cation radical metalloporphyrin species. The relative ease in preparing the mixed-valence π-cation radicals demonstrates the stability resulting from delocalization of the π-radical electron hole over more than one porphyrin ring.

Experimental Section

General Information. H_2OEP was purchased from Midcentury Chemicals, Pd(OEP), thianthrene, perchloric acid, tris(4-bromophenyl)-aminium hexachloroantimonate, and CCl_4 were purchased from Aldrich, and all other reagents were obtained from Fisher. Dichloromethane and hexane were distilled from CaH_2 and sodium/benzophenone, respectively. All reactions were performed under an argon atmosphere with oven-dried Schlenkware and cannula techniques. Except for Pd(OEP), metals were inserted into the free-base H_2OEP by standard techniques.[18,19] CH_2Cl_2 solutions for equilibrium measurements were prepared using volumetric glassware. Absorption spectra samples were placed in a Teflon-stoppered quartz mixing cell (total path length 0.87 cm) and recorded on a Perkin-Elmer Lambda 19 UV/vis/near-IR spectrometer. Thianthrenium perchlorate was prepared by literature procedures.[20] *Caution!* Perchlorate salts can detonate spontaneously and should be handled only in milligram quantities; other safety precautions are also warranted.[21]

Preparation of [M(OEP$^{\bullet}$)][ClO_4], M = Cu, Ni, Zn, or Pd. Cu(OEP) (60 mg, 0.101 mmol) and thianthrenium perchlorate (33 mg, 0.105 mmol) were placed in a 100-mL Schlenk flask. Dichloromethane (~50 mL) was added through a cannula and the solution was stirred for 1 h. The volume was reduced to ~10 mL by vacuum evaporation, and hexane was added to induce precipitation. The precipitate was filtered under argon and allowed to dry under vacuum for several hours (yield 76%). UV/vis/near-IR (CH_2Cl_2): λ_{max} 380 (Soret), 512, 563, 614, 914 nm. IR (KBr): ν(OEP$^{\bullet}$) 1595 cm^{-1} (strong). Other π-cation radical derivatives were prepared in the same fashion as the copper complexes. [Ni(OEP$^{\bullet}$)][ClO_4]: UV/vis/near-IR (CH_2Cl_2) λ_{max} 386 (Soret), 571, 637, 905 nm; IR (KBr) ν(OEP$^{\bullet}$) 1568 cm^{-1} (strong); yield 73%. [Zn(OEP$^{\bullet}$)][ClO_4]: UV/vis/near-IR (CH_2Cl_2) λ_{max} 386 (Soret), 571, 637, 955 nm; IR (KBr) ν(OEP$^{\bullet}$) 1530, 1555 cm^{-1} (weak, doublet); yield 78%. [Pd(OEP$^{\bullet}$)][ClO_4]: UV/vis/near-IR (CH_2Cl_2) λ_{max} 375 (Soret), 511, 574, 930 nm; yield 73%.

Preparation of [M(OEP$^{\bullet}$)][$SbCl_6$], M = Cu, Ni, Zn, VO, or Pd. Cu(OEP) (60 mg, 0.101 mmol) in ~ 50 mL of CH_2Cl_2 was reacted with tris(4-bromophenyl)aminium hexachloroantimonate (86 mg, 0.105 mmol) in a 100-mL Schlenk flask. After the mixture was stirred for 1 h, the volume was reduced to ~15 mL. The solution was then transferred from the reaction vessel Schlenk flask into a 50-mL Schlenk flask by a cannula and then layered with hexane for crystallization. The dark purple crystals that formed after ~4 days were washed with hexane and allowed to dry (yield 77%). UV/vis/near-IR (CH_2Cl_2): λ_{max} 381 (Soret), 512, 562, 614, 914 nm. IR (KBr): ν(OEP$^{\bullet}$) 1580 cm^{-1} (strong). The other hexachloroantimonate π-cation radical salts were similarly prepared. [Ni(OEP$^{\bullet}$)][$SbCl_6$]: UV/vis/near-IR (CH_2Cl_2) λ_{max} 375 (Soret), 501, 575, 911 nm; IR (KBr) ν(OEP$^{\bullet}$) 1571 cm^{-1} (strong); yield 75%. [Zn(OEP$^{\bullet}$)][$SbCl_6$]: UV/vis/near-IR (CH_2Cl_2) λ_{max} 391

(14) (a) Senge, M. O.; Vicente, M. G. H.; Gerzevske, K. R.; Forsyth, T. P.; Smith, K. M. *Inorg. Chem.* **1994**, *33*, 5625. (b) Pascard, C.; Guilhem, J.; Chardon-Noblat, S.; Sauvage, J.-P. *New J. Chem.* **1993**, *17*, 331. (c) Le Mest, Y.; L'Her, M.; Hendricks, N. H.; Kim, K.; Collman, J. P. *Inorg. Chem.* **1992**, *31*, 835. (d) Osuka, A.; Nagata, T.; Maruyama, K. *Chem. Lett.* **1991**, 481. (e) Osuka, A.; Nakajima, S.; Nagata, T.; Maruyama, K.; Toriumi, K. *Angew. Chem., Int. Ed. Engl.* **1991**, *30*, 582. (f) Rodriguez, J.; Kirmaier, C.; Johnson, M. R.; Friesner, R. A.; Holten, D.; Sessler, J. L. *J. Am. Chem. Soc.* **1991**, *113*, 1652. (g) Sessler, J. L.; Johnson, M. R.; Creager, S. E.; Fettinger, J. C.; Ibers, J. A. *J. Am. Chem. Soc.* **1990**, *112*, 9310. (h) Cowan, J. A.; Sanders, J. K. M.; Beddard, G. S.; Harrison, R. J. *J. Chem. Soc., Chem. Commun.* **1987**, 55. (i) Dubowchik, G. M.; Hamilton, A. D. *J. Chem. Soc., Chem. Commun.* **1986**, 1391.

(15) (a) Buchler, J. W.; Knoff, M. In *Optical Properties and Structure of Tetrapyrroles*; Blauer, G., Sund, H., Eds.; de Gruyter: West Berlin, 1985; pp 91−105. (b) Buchler, J. W.; Elsässer, K.; Kihn-Botulinski, M.; Scharbert, B. *Angew. Chem.* **1986**, *98*, 257. (c) Girolami, G. S.; Milam, S. N.; Suslick, K. S. *J. Am. Chem. Soc.* **1988**, *110*, 2011. (d) Buchler, J. W.; Scharbert, B. *J. Am. Chem. Soc.* **1988**, *110*, 4272. (e) Donohoe, R. J.; Duchowski, J. K.; Bocian, D. F. *J. Am. Chem. Soc.* **1988**, *110*, 6119. (f) Buchler, J. W.; De Cian, A.; Fischer, J.; Hammerschmitt, P.; Löffler, J.; Scharbert, B.; Weiss, R. *Chem. Ber.* **1989**, *122*, 2219. (g) Duchowski, J. K.; Bocian, D. F. *J. Am. Chem. Soc.* **1990**, *112*, 3312. (h) Bilsel, O.; Buchler, J. W.; Hammerschmitt, P.; Rodriguez, J.; Holten, D. *Chem. Phys. Lett.* **1991**, *182*, 415. (i) Kim, H.-J.; Whang, D.; Kim, J.; Kim, K. *Inorg. Chem.* **1992**, *31*, 3882. (j) Girolami, G. S.; Gorlin, P. A.; Suslick, K. S. *Inorg. Chem.* **1994**, *33*, 626. (k) Girolami, G. S.; Gorlin, P. A.; Milam, S. N.; Suslick, K. S.; Wilson, S. R. *J. Coord. Chem.* **1994**, *32*, 173.

(16) Scheidt, W. R.; Cheng, B.; Haller, K. J.; Mislanker, A.; Rae, A. D.; Reddy, K. V.; Song, H.; Orosz, R. D.; Reed, C. A.; Cubiernik, F.; Marchon, J. C. *J. Am. Chem. Soc.* **1993**, *115*, 1181.

(17) Scheidt, W. R.; Brancato-Buentello, K. E.; Song, H.; Reddy, K. V.; Cheng, B. *Inorg. Chem.* **1996**, *35*, 7500.

(18) Adler, A. D.; Longo, F. R.; Kampas, F.; Kim, J. *J. Inorg. Nucl. Chem.* **1970**, *32*, 2443.

(19) Schulz, C. E.; Song, H.; Lee, Y. J.; Mondal, J. U.; Mohanrao, K.; Reed, C. A.; Walker, F. A.; Scheidt, W. R. *J. Am. Chem. Soc.* **1994**, *116*, 7196.

(20) Murata, Y.; Shine, H. *J. Org. Chem.* **1969**, *34*, 3368.

(21) Wolsey, W. C. *J. Chem. Educ.* **1973**, *50*, A335. *Chem. Eng. News* **1983**, *61* (Dec. 5), 4; **1963**, *41* (July 8), 47.

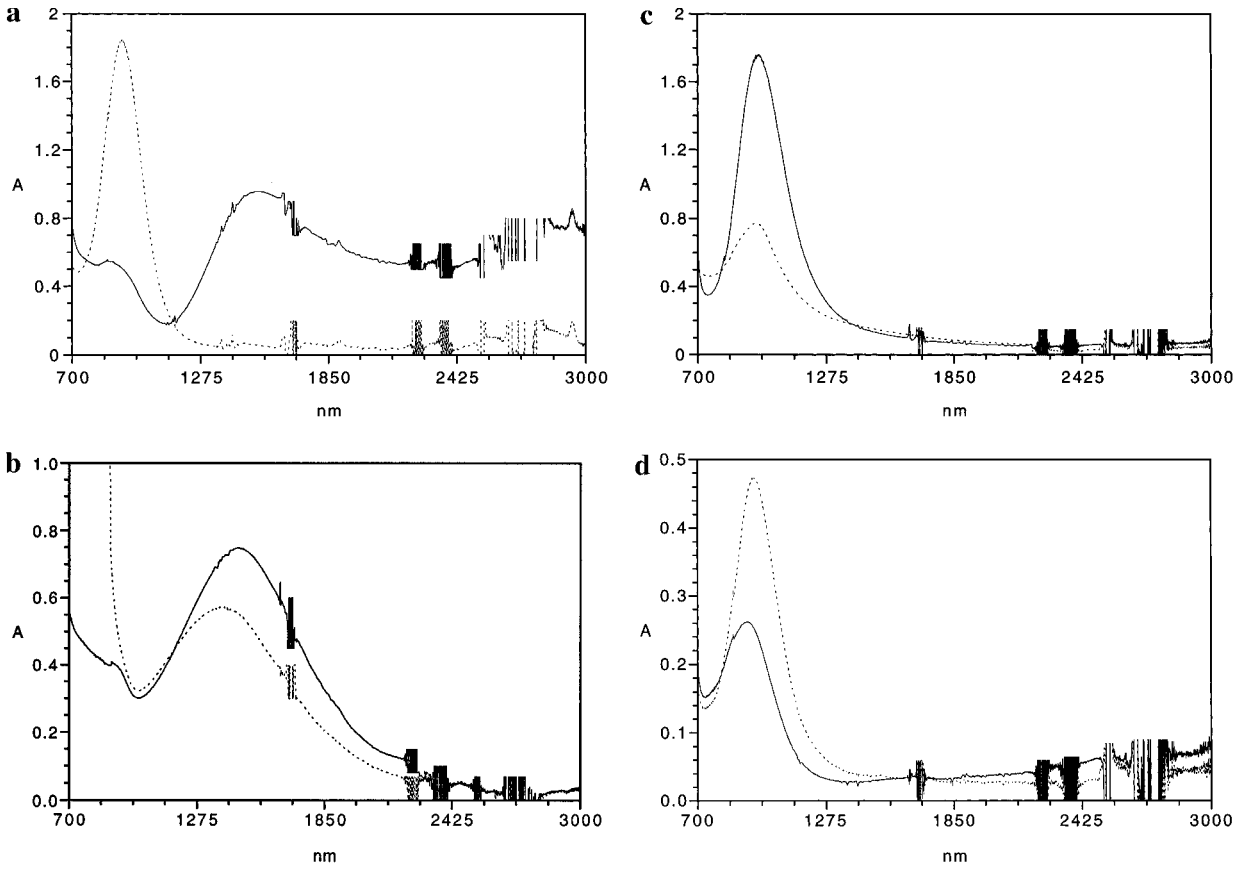

Figure 1. Spectral sum (700−3000 nm) of equimolar solutions of M(OEP) and [M(OEP•)]Y held in the two compartments of a mixing cuvette ("before reaction" spectra (- - -)). "After reaction" spectra (—) are obtained after the two solutions are mixed; these spectra are virtually identical with that of pure $[M(OEP^{\bullet/2})]_2Y$. The oscillations at wavelengths greater than 1600 nm result from interference of CH_2Cl_2. (a) M = Cu, Y = $SbCl_6$, concentration = 2.0×10^{-3} M; (b) M = VO, Y = $SbCl_6$, concentration = 2.0×10^{-3} M; (c) M = Zn, Y = $SbCl_6$, concentration = 8.0×10^{-4} M; (d) M = Zn, Y = ClO_4, concentration = 6.67×10^{-4} M.

(Soret), 534, 559, 596, 651, 960 nm; yield 72%. $[VO(OH_2)(OEP^{\bullet})][SbCl_6]$: UV/vis/near-IR ($CH_2Cl_2$) λ_{max} 391 (Soret), 474 (sh), 515, 622, 1375 nm; IR (KBr) ν(OEP•) 1533 cm^{-1} (strong); yield 74%. $[Pd(OEP^{\bullet})][SbCl_6]$: UV/vis/near-IR ($CH_2Cl_2$) λ_{max} 375 (Soret), 509, 575, 928 nm; IR (KBr) ν(OEP•) 1582 cm^{-1} (strong); yield 70%.

Preparation of $[Pd(OEP^{\bullet/2})]_2[ClO_4]$. Pd(OEP) (70 mg, 0.101 mmol) and thianthrenium perchlorate (17 mg, 0.055 mmol) were placed in a 100-mL Schlenk flask. Dichloromethane (∼75 mL) was added through a cannula and the solution was stirred for 1 h. The volume was reduced to ∼10 mL by vacuum evaporation, and hexane was added to induce precipitation. The precipitate was filtered under argon and allowed to dry under vacuum for several hours (yield 80%). UV/vis/near-IR (CH_2Cl_2) 392 (Soret), 512, 545, 1471 nm; IR (KBr) ν(OEP•) 1674 cm^{-1} (weak).

Preparation of $[Pd(OEP^{\bullet/2})]_2[SbCl_6]$. Pd(OEP) (70 mg, 0.101 mmol) in ∼75 mL of CH_2Cl_2 was reacted with tris(4-bromophenyl)-aminium hexachloroantimonate (45 mg, 0.055 mmol) in a 100-mL Schlenk flask. After the mixture was stirred for 1 h, the volume was reduced to ∼15 mL. The solution was then transferred from the reaction vessel Schlenk flask into a 50-mL Schlenk flask by a cannula and then layered with hexane for crystallization. The dark purple crystals that formed after ∼4 days were washed with hexane and allowed to dry (yield 76%). UV/vis/near-IR (CH_2Cl_2) 392 (Soret), 512, 546, 1472 nm.

Equilibrium Constant Determinations. All equilibrium constant measurements, except those involving the palladium complexes,[22] were conducted by titration of the neutral complex and the π-cation radical in a quartz mixing cell. CH_2Cl_2 solutions of neutral, M(OEP), and the π-cation radical, [M(OEP•)]Y, were each placed in one of the compartments of a Teflon-stoppered quartz mixing cell (total path length = 0.87 cm). Eight different concentrations of the neutral complex and the π-cation radical were used in a typical experiment. Most experiments used the same concentrations for the two species, but some experiments were also performed in which the concentration of the two were different by factors of 1.5 or 2. The "before reaction" spectra were recorded from 700 to 3000 nm. The cell was then inverted, the two solutions were mixed thoroughly, and an "after reaction" spectrum was taken over the same spectral range. A new near-IR band is observed in all after reaction spectra. Table 1 presents the range of before reaction concentrations used along with wavelength maxima for

Table 1. Summary of Spectral Maxima for the M(OEP), [M(OEP•)]Y, and $[M(OEP^{\bullet/2})]_2Y$ Systems Including Concentration Ranges Studied

			λ_{max}, nm[a]	
M	Y	concn range ($\times 10^{-3}$ M)	"before reaction"	"after reaction"
Ni	$SbCl_6$	2.00−0.25	911	1540
Ni	ClO_4	2.00−0.25	905	1537
Cu	$SbCl_6$	2.00−0.25	914	1541
Cu	ClO_4	2.00−0.25	914	1529
Pd	$SbCl_6$	1.20−0.15	928	1472
Pd	ClO_4	1.20−0.15	930	1471
Zn	$SbCl_6$	0.80−0.16	960	974
Zn	ClO_4	0.80−0.16	955	925
VO	$SbCl_6$	1.30−0.16	1375	1446
H_2,Zn	$SbCl_6$	0.60−0.15	960	930
Ni,Cu	$SbCl_6$	2.00−0.25	914	1527
Cu,Ni	$SbCl_6$	2.00−0.25	909	1525

[a] Relative uncertainties in absorption maxima are estimated to be ∼5 nm. All spectra were measured in methylene chloride solution.

(22) Neutral Pd(OEP) is minimally soluble in CH_2Cl_2, and therefore, mixing experiment titrations could not be carried out. Rather, various concentrations of π-cation radical solutions were prepared directly, equilibrium measurements were carried out as they were for the other metallo systems, and the procedure was repeated for the mixed valence π-cation radical complexes.

the before and after reaction species. Typical before and after reaction spectra, in the near-IR region for M = Cu, are shown in Figure 1a.

The after reaction spectra primarily reflect the reaction:

$$M(OEP) + [M(OEP^{\bullet})]^{+} \overset{K_{MV}}{\rightleftharpoons} [M(OEP^{\bullet/2})]_2^{+} \quad (1)$$

although due consideration of the additional equilibrium

$$2[M(OEP^{\bullet})]^{+} \overset{K_{D}}{\rightleftharpoons} [M(OEP^{\bullet})]_2^{2+} \quad (2)$$

must be made for completeness of the analysis. The value of this second equilibrium constant can be evaluated independently by an analysis of the before reaction spectra or direct measurements.

The equilibrium constants for these equilibria were calculated with the nonlinear least-squares program SQUAD[23] on a DEC VAXstation 4000−90A. SQUAD calculates best values for the equilibrium constants by employing multiple-wavelength absorption data for varying concentrations of the reactants. A particularly useful feature of SQUAD is that it can accommodate multiple equilibria. Absorbance data, at 30−50-nm increments spanning the near-IR region, were input into SQUAD. Computation of K_D, eq 2, used the absorbance data from the before reaction spectra.[24] The extinction coefficients for the monomer and dimer radicals over the entire spectral range (700−3000 nm) were then calculated using this K_D. The after reaction absorbance data were then used to calculate K_{MV}, eq 1, while holding K_D and the associated extinction coefficients fixed at the values determined in the first step.

Selected equilibrium constants were determined as a function of temperature over a 23 or 34 deg temperature range. Temperature control was provided by a Fisher Scientific Model 900 Isotemp Refrigerated Circulator bath. The solution temperatures were measured using an Omega Model 199 series digital thermometer fitted with an iron−constantan thermocouple immersed in the solutions. Van't Hoff plots were then used to estimate the values of the enthalpy and entropy of formation.

Results

The reaction of equimolar dichloromethane solutions of the π-cation radical $[M(OEP^{\bullet})]^{+}$ and neutral M(OEP) leads to the appearance of a new, broad, near-IR band in the electronic spectrum. The near-IR absorption maxima are listed in Table 1 ("after reaction") for a number of different systems with varying metal and anion. We associate the new near-IR band with the formation of a novel species, $[M(OEP^{\bullet/2})]_2^{+}$, which is in equilibrium with the starting species:

$$M(OEP) + [M(OEP^{\bullet})]^{+} \overset{K_{MV}}{\rightleftharpoons} [M(OEP^{\bullet/2})]_2^{+} \quad (1)$$

The constant for this equilibrium process can be determined by an analysis of "mixing experiment" spectral titrations; these calculated values are listed in Table 2. Another near-IR band, which is associated with the π-cation radical (Table 1, "before reaction"), diminishes in intensity upon reaction. This near-IR band is associated with a dimerization of the π-cation radical:

$$2[M(OEP^{\bullet})]^{+} \overset{K_{D}}{\rightleftharpoons} [M(OEP^{\bullet})]_2^{2+} \quad (2)$$

Again, an equilibrium constant can be determined from an analysis of the spectral data and the constants are listed in Table 3. The quoted equilibrium constants are based on at least duplicate determinations. Although the agreement in the value of K's between runs was quite good, the values of the variances between sets of measurements showed larger spreads. Accordingly, we have calculated weighted means and weighted variances[25] rather than simple averages and these weighted values are reported in Tables 2 and 3.

We have also determined K_{MV} and K_D values over a range of temperature. The temperature of the experiments was restricted to the range −13 to 20 °C, because of the need to use dichloromethane as solvent and the limited solubility at lower temperatures. Nonetheless, the van't Hoff plots were linear (linear correlation coefficients > 0.99) with reasonably large slopes. Table 4 gives enthalpy and entropy parameters derived from the van't Hoff plots for both equilibrium processes.

We have also prepared and isolated a number of the mixed-valence π-cation radical species as crystalline solids. The spectra obtained by dissolving these isolated complexes are identical to those obtained above by mixing experiments. We

Table 2. Equilibrium Constants (log K_{MV}, 291 K) for the following Reaction[a]

$$M(OEP) + [M'(OEP^{\bullet})]Y \overset{K_{MV}}{\rightleftharpoons} [M,M'(OEP^{\bullet/2})_2]Y$$

M	M′	Y	log K_{MV}
Ni	Ni	$SbCl_6$	3.18 ± 0.05
Ni	Ni	ClO_4	3.19 ± 0.05
Cu	Cu	$SbCl_6$	3.72 ± 0.03
Cu	Cu	ClO_4	3.78 ± 0.05
Ni	Cu	$SbCl_6$	3.58 ± 0.01
Cu	Ni	$SbCl_6$	3.54 ± 0.04
Pd	Pd	$SbCl_6$	3.39 ± 0.07
Pd	Pd	ClO_4	3.42 ± 0.10
Zn	Zn	$SbCl_6$	4.31 ± 0.09
Zn	Zn	ClO_4	3.77 ± 0.04
VO	VO	$SbCl_6$	4.00 ± 0.12
H_2	Zn	$SbCl_6$	3.2 ± 0.3

[a] All reactions in CH_2Cl_2.

Table 3. Equilibrium Constants (log K_D, 291 K) for the Reaction[a]

$$2[M(OEP^{\bullet})]Y \overset{K_{D}}{\rightleftharpoons} [M(OEP^{\bullet})]_2Y_2$$

M	Y	log K_D
Ni	$SbCl_6$	2.00 ± 0.06
Ni	ClO_4	1.75 ± 0.09
Cu	$SbCl_6$	2.09 ± 0.07
Cu	ClO_4	2.02 ± 0.03
Pd	$SbCl_6$	2.73 ± 0.06
Pd	ClO_4	3.05 ± 0.06
Zn	$SbCl_6$	2.68 ± 0.11
Zn	ClO_4	2.30 ± 0.18
VO	$SbCl_6$	2.40 ± 0.09

[a] All reactions in CH_2Cl_2.

Table 4. Experimental Enthalpy and Entropy Values in Methylene Chloride Solution

M	chemical species[a]	ΔH (kcal/mol)	ΔS (cal/(mol·K))	ref
Ni	dimer	−11	−28	this work
Cu	dimer	−8.4	−20	this work
Zn	dimer	−18	−38	30[b]
VO	dimer	−5.6	−9.5	this work
Ni	mixed-valence	−5.7	−4.9	this work
Cu	mixed-valence	−6.8	−5.6	this work
Zn	mixed-valence	−6.8	−3.1	this work
VO	mixed-valence	−6.8	−4.9	this work

[a] Dimer is the formation of $[M(OEP^{\bullet})]_2^{2+}$; mixed-valence is the formation of $[M(OEP^{\bullet/2})]_2^{+}$. [b] Measured in MeOH:$CHCl_3$ (10:1).

(23) Leggett, D. J. In Computational Methods for the Determination of Formation Constants; Leggett, D. J., Ed.; Plenum: New York, 1985; Chapter 6.

(24) The spectral range used initially included the entire main portion of the peak (a range of ~450 nm). There is no contribution to the absorbance from M(OEP) over the near-IR spectral region.

(25) Hamilton, W. C. *Statistics in Physical Sciences*; Ronald: New York, 1964; pp 37−42.

suggest the term "mixed-valence π-cation radical" for these new compounds.

Discussion

Solution Equilibria. The initial preparations of species with the chemical formula $[M(OEP^{\bullet/2})]_2^+$ were accomplished by the oxidation of metalloporphyrin derivatives with 0.5 equiv of an appropriate one-electron oxidant and were isolated as crystalline solids. Structural analyses[16,17] of crystalline species show that the compounds exist as discrete binuclear units in the solid. The stability of such species in solution might have been expected to be rather minimal with decomposition readily occurring by disproportionation:

$$[M(OEP^{\bullet/2})]_2^+ \overset{K_{disp}}{\rightleftharpoons} M(OEP) + [M(OEP^{\bullet})]^+$$

However, the reverse reaction, the comproportionation reaction, written previously as eq 1, actually dominates the solution chemistry of a mixture of the neutral and π-cation radical metallooctaethylporphyrins; the equilibrium position of such reactions largely favors the mixed-valence species $[M(OEP^{\bullet/2})]_2^+$. We have denoted the comproportionation constants as K_{MV} throughout this paper.

Values of K_{MV} have been determined for a number of different systems in which the metal ion and/or the counterion were varied. The magnitudes of K_{MV} are moderately large and range from ~1600 to ~20 000. A complete listing of determined K_{MV} values is given in Table 2. There are a number of features to be noted. For the Ni, Cu, and Pd systems, where the metal ions are expected to remain four coordinate, the formation constants are independent of the choice of the counterion, hexachloroantimonate or perchlorate ion. For the zinc systems, where the zinc ion has an affinity for a possible axial ligand, there is a dependence on the counterion. Thus the differences in K_{MV} for the two zinc systems can be attributed to whether or not the counterion ligates the central zinc atom. We have attempted to keep all systems anhydrous; however, we should note that in the zinc and vanadyl systems, the presence of water could have an effect on the equilibrium constants. Both metals are known to form aquated π-cation radicals[19,26] and there are apparent differences in axial ligand affinity between the neutral and π-cation porphyrins.

Finally it is to be noted that the mixed-valence π-cation radical formation constants show variation with the central metal ion. The solid-state structures,[16,17] and the likely solution structures, have as their most important inter-ring attractive interaction a π−π interaction; the metal···metal distances are larger than that expected for a significant metal−metal bond interaction. The strengths of these π−π links are surely related, *inter alia*, to the energies of the HOMO and LUMO orbitals, which are known[27] to be metal dependent. Thus a modest dependence on metal ion identity in the various derivatives is reasonably expected.

Values of K_{MV} for a limited number of mixed-valence hetero systems (in which the two metals are different) have also been determined. For the Ni/Cu systems, the two formation constants are equal—independent of whether the reacting π-cation radical is $[Ni(OEP^{\bullet})]^+$ or $[Cu(OEP^{\bullet})]^+$. The resulting spectroscopic properties of the two Ni/Cu mixed systems are also indistinguishable from each other. Moreover, the final spectroscopic properties of the mixed Ni/Cu systems are distinct from either the purely nickel or purely copper system. We can thus conclude that a mixed metalloporphyrin system indeed results and that its preparation is independent of reaction path.[28] The fact that a new product is formed in these Ni/Cu mixed systems suggests that the unpaired electron must be delocalized over both metalloporphyrin rings. However, the unpaired electron may not be delocalized equally over the two rings in mixed systems; any asymmetry in electron delocalization would be related to differences in the ring oxidation potentials. It is interesting to note that the two K_{MV} values for the mixed Ni/Cu system (Table 2) are quite close, but perhaps not exactly equal, to the arithmetic mean of the homo nickel and copper systems; the deviation from the exact mean may indicate asymmetry in the electron delocalization. This issue is under active consideration.

We have also determined the formation constant for the mixed Zn(OEP), free base species which we write as $[Zn(OEP^{\bullet/2})\text{-}H_2(OEP^{\bullet/2})]^+$; the $\log(K_{MV})$ value is a respectable 3.2. In this case the mixing experiments could be successfully performed only by reaction of $[Zn(OEP^{\bullet})]^+$ with H_2OEP and not the reverse. It is not immediately clear to us why this is so, since it is easier to oxidize Zn(OEP) than H_2OEP; the difference in the first ring oxidation potential is at least 180 mV.[29] Thus the most likely explanation for the reactivity difference would appear to be mechanistic, rather than thermodynamic, in origin.

We find that in methylene chloride solution all $[M(OEP^{\bullet})]^+$ π-cation radicals exhibit a near-IR absorption band whose intensity is strongly concentration dependent. The behavior of this band is that expected for the dimeric species of a monomer−dimer equilibrium:

$$2[M(OEP^{\bullet})]^+ \overset{K_D}{\rightleftharpoons} [M(OEP^{\bullet})]_2^{2+}$$

The concentration dependence of the near-IR spectra of $[M(OEP^{\bullet})]^+$ species can be readily used to obtain values for the dimerization formation constants K_D, which are listed in Table 3. Although the thermodynamics of the dimerization of $[Zn(OEP^{\bullet})]Br$ was studied two decades ago,[30] to our knowledge no other quantitative measurements have been made for any porphyrin radical derivatives. However, temperature-dependent electronic spectral and EPR studies have shown that vanadyl,[19] magnesium,[31] and copper[32] derivatives undergo strongly coupled dimerization reactions in solution. In our experience this dimerization is the norm. The data in Table 3 show that palladium species have even larger dimerization constants than the zinc derivatives. This may be related to the strong tendency for even neutral Pd(OEP) to aggregate and to have limited solubility.

In all cases the mixed-valence π-cation formation constants (K_{MV}) are significantly larger (by a factor of 10 to 100) than the analogous dimerization constants K_D. Such differences are, of course, consistent with the observation of the importance of the comproportionation pathway over disproportionation in reactions of the π-cation radicals. The observation further suggests significant stabilization from the delocalization of a

(26) Song, H.; Orosz, R. D.; Reed, C. A.; Scheidt, W. R. *Inorg. Chem.* **1990**, *29*, 4274.

(27) Zerner, M.; Gouterman, M.; Koboyashi, H. *Theor. Chim. Acta* **1966**, *6*, 363.

(28) The absorbance values from the mixed metal reactions are clearly incompatible with the presence of only the homonuclear dimers in any proportions.

(29) Measurement in butyronitrile: Fuhrhop, J.-H.; Kadish, K. M.; Davis, D. G. *J. Am. Chem. Soc.* **1973**, *95*, 5140. A measurement in methylene chloride gave a difference slightly larger: K. Brancato-Buentello, unpublished observations.

(30) Fuhrhop, J. H.; Wasser, P.; Riesner, D.; Mauzerall, D. *J. Am. Chem. Soc.* **1972**, *94*, 7996.

(31) Fajer, J.; Borg, D. C.; Forman, A.; Dolphin, D.; Felton, R. H. *J. Am. Chem. Soc.* **1970**, *92*, 3451.

(32) (a) Mengersen, C.; Subramanian, J.; Fuhrhop, J.-H. *Mol. Phys.* **1976**, *32*, 893. (b) Browett, W. R.; Stillman, M. J. *Inorg. Chim. Acta* **1981**, *49*, 69.

single radical electron over two porphyrin rings in the mixed-valence π-cations.

We have further explored the differences in these two reactions by determining the values of ΔH and ΔS, which were evaluated by the van't Hoff method. The necessary use of methylene chloride as solvent limits the temperature range available for the study, but the data appear adequate to define trends. Values of ΔH and ΔS are listed in Table 4. Two generalizations are apparent. The reaction enthalpies are favorable for both reactions. The formation of π-cation radical dimers is the more enthalpically favored process as might be expected; however, the reaction enthalpies differ by less than a factor of two. The reaction entropies are all negative as might be expected for dimerization reactions. The formation of π-cation radical dimers leads to reaction entropies that are much more negative than those for the formation of the mixed-valence π-cation radicals. Indeed the reaction entropies differ by factors near 5. This must result from a much larger solvent reorganization that occurs in the π-cation radical dimerization reaction. Importantly, the overall greater thermodynamic stability of the mixed-valence π-cation radicals can be directly attributed to the reaction entropy differences.

Electronic Spectra. Two species of prime interest in this study, the mixed-valence π-cation radical octaethylporphyrin species, $[M(OEP^{\bullet/2})]_2^+$, and the π-cation radical octaethylporphyrin dimers, $[M(OEP^{\bullet})]_2^{2+}$, exhibit broad bands in the near-IR portion of the electromagnetic spectrum. Positions of the near-IR maxima have been given in Table 1: the "before reaction" column corresponds to the spectrum of π-cation radical dimers and the "after reaction" column to the spectrum of mixed-valence π-cation radical complexes. Owing to the broadness of the near-IR bands the reported maxima are probably accurate to no better than $\sim$5 nm. The other species involved in the equilibria described above, viz., neutral metallooctaethylporphyrins and monomeric π-cation radicals, do not absorb significantly in the near-IR region.

Representative spectra (four systems) for the near-IR region are shown in Figure 1. The bands represented by the dashed lines (the "before reaction" spectra) are from the absorption of the dimeric π-cation radical species, $[M(OEP^{\bullet})]_2^{2+}$. This band occurs in the near-IR region at 900−960 nm except for the vanadyl derivative, which has a significantly red-shifted band. In all cases the apparent extinction coefficient of this band is strongly concentration dependent. As noted earlier, the concentration dependence of the band can be quantitatively explained by a dimerization reaction in which the dimer absorbs much more strongly than the monomer. The position of the near-IR bands is similar to the band assigned by Fuhrhop et al.[30] and Fajer et al.[31] as resulting from dimerization in the $[Zn(OEP^{\bullet})]^+$ and $[Mg(OEP^{\bullet})]^+$ radical systems, respectively. It is important to note that the solution dimerization of the metallooctaethylporphyrin π-cation radicals and the concomitant appearance of a near-IR band appears to be much more prevalent than has been previously recognized. Interestingly however, the π-cation radical of the parent free base $[H_2(OEP^{\bullet})]^+$ shows neither a near-IR band nor the expected concentration-dependent blue-shifted Soret band. Both of these spectral features accompany π-cation radical dimer formation. Thus, there is no spectral evidence for the formation of free base radical dimers.

The simplest electronic structure model that can be used to understand dimerization of π-cation radicals can be schematically depicted as shown in Figure 2.[33] The half-filled molecular

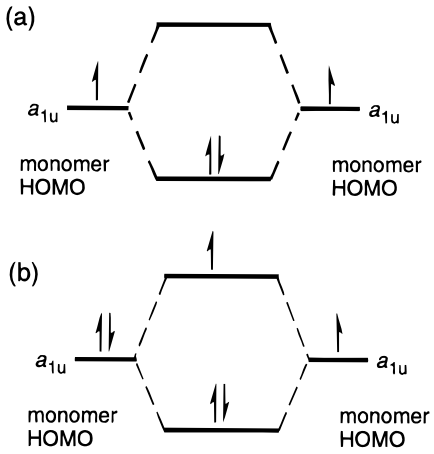

Figure 2. Simplified bonding scheme for formation of binuclear (a) π-cation and (b) mixed-valence π-cation radical species.

orbital of a monomeric metallooctaethylporphyrin π-cation radical is, in D_{4h} symmetry, an a_{1u} orbital. Two such orbitals, one from each monomer, can combine to form a new "bonding" and a new "antibonding" molecular orbital that are delocalized over both porphyrin rings in the resultant dimer. Such a simple bonding picture is consistent, for example, with the known solid-state diamagnetism of the $[Zn(OEP^{\bullet})]_2^{2+}$ dimer.[26] In this simple model, the assignment of the near-IR dimerization band is that of excitation from the bonding to the antibonding molecular orbital. Knowledge of the excitation energy then allows an estimate of the enthalpy of formation: it must be nominally less than half the excitation energy. This expectation is qualitatively met, with the spectroscopic transition energies for the nickel, copper, and zinc systems at 30−31 kcal/mol and with the measured enthalpies for the nickel and copper systems approximately one-third as large. A similar pattern is seen in the vanadyl radical system, where the red-shifted transition has an energy of 21 kcal/mol and the measured dimerization enthalpy is 6 kcal/mol. The zinc system, where the enthalpy was measured in a different (more polar) solvent system, has a value a bit greater than half that of the measured excitation energy.

The electronic spectra of the new, related mixed-valence species, $[M(OEP^{\bullet/2})]_2^+$ (represented by the solid lines in Figure 1), also have distinct near-IR bands. The near-IR band is frequently shifted to the red relative to the band observed for the related dimeric π-cation radical species. A significant spectral red shift is displayed in the copper, nickel, palladium, and mixed copper/nickel systems. This is illustrated in Figure 1a for the copper system. Also apparent in the displayed spectrum is the strong tailing of the near-IR band farther into the infrared. This tailing is especially prominent in the nickel and copper cases, where the tailing continues into the infrared. The tailing even leads to anomalously high backgrounds in the IR spectra of $[M(OEP^{\bullet/2})]_2^+$, M = Cu or Ni (KBr pellets, high backgrounds down to $\sim$1600 cm^{-1}). The position of the near-IR band in the mixed-valence zinc systems, however, shows relatively small shifts compared to the band position observed for the radical cation dimers. Moreover, as can be seen in Figures 1c and 1d, there is a strong anion dependence on the intensity of the bands in the different species, which may reflect differences in axial ligation. The near-IR maxima of the π-cation and mixed-valence π-cation radical vanadyl systems also show only small differences, but both are quite red-shifted compared to the zinc systems (cf. Figure 1b). As can be seen from the displayed spectra in Figures 1b−d, these latter compounds do not have strongly tailed near-IR bands. The most

(33) More detailed MO bonding models for lanthanide double-deckers that encompass these combinations of the a_{1u} orbitals have been given previously. See refs 15e,g,h.

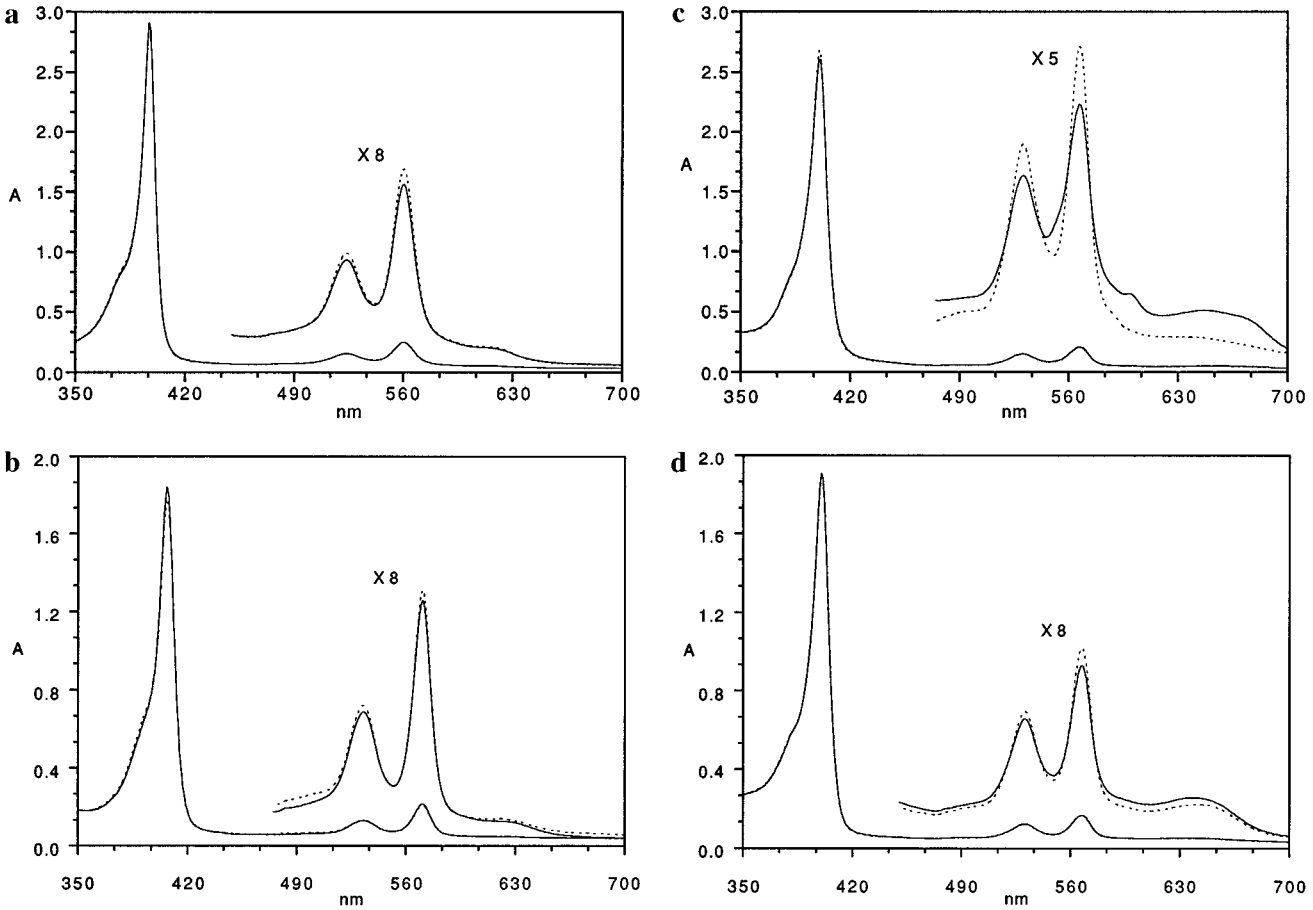

Figure 3. Spectral sum (350−700 nm) of equimolar solutions of M(OEP) and [M(OEP•)]Y held in the two compartments of a mixing cuvette ("before reaction" spectra (- - -)). "After reaction" spectra (—) are obtained after the two solutions are mixed; these spectra are identical with that obtained from pure $[M(OEP^{\bullet/2})]_2Y$. (a) M = Cu, Y = $SbCl_6$, concentration = 9.37×10^{-6} M (Soret), 7.5×10^{-5} M (vis); (b) M = VO, Y = $SbCl_6$, concentration = 9.37×10^{-6} M (Soret), 7.5×10^{-5} M (vis); (c) M = Zn, Y = $SbCl_6$, concentration = 6.25×10^{-5} M (Soret), 2.5×10^{-4} M (vis); (d) M = Zn, Y = ClO_4, concentration = 9.37×10^{-6} M (Soret), 7.5×10^{-5} M (vis).

reasonable spectral assignment of these near-IR bands is one related to that given earlier for the π-cation dimers (Figure 2). The mixed-valence π-cation radicals have one additional electron which must be placed in the "antibonding" combination; the near-IR transition is thus the one between the second-highest occupied molecular orbital (SHOMO) and the singly occupied HOMO.

The near-IR bands of the mixed-valence π-cation radicals resemble the new near-IR band that appears when bacterial photosynthetic reaction centers, e.g., those from *Rhodopseudomonas viridis* or *Rhodobacter sphaeroides*, are photooxidized[6a,34−37] and form the oxidized special pair, P^+. A common assignment of the near-IR transitions would seem probable. The assignment of this near-IR band for P^+ remains a matter of current interest.[38] Stocker et al.[39] present strong evidence for the band arising from an electronic transition between states completely delocalized over the two rings on the vibrational and electronic time scales. The delocalized states of P^+ would be consistent with a SHOMO → HOMO transition. However, Reimers and Hush[38] favor another assignment based on calculations of expected intensities. They further note that their calculations suggest that the near-IR bands in analogous lanthanide double-deckers are only coincidently similar to that of P^+. The mixed-valence π-cation radical near-IR band is unlikely to be an optical hole transition between the two porphyrin rings, i.e., the classic intervalence transfer band. A lower energy band has been recently found by difference spectroscopy for P^+ in the mid-IR;[40] this appears to be the intervalence transfer band. While the current study does not attempt to present an unequivocal assignment of the near-IR bands, it clearly shows that geometrically unconstrained dimers can display near-IR bands. The mixed-valence π-cation radical systems provide a new basis for the exploration of effects of inter-ring geometry and metal variation on the spectroscopic properties.

The spectral features in the UV−vis region of all the π-cation radicals investigated here are similar to those reported by Fuhrhop et al.[30] for the $[Zn(OEP^{\bullet})]_2^{2+}$ dimer. In the dimer spectra, the Soret band is weaker, blue-shifted, and broadened compared to the neutral precursors while the α and β bands of the π-cation radicals are red-shifted as well as substantially broadened. There is, of course, a concentration dependence in these spectra consistent with the dimerization process.

The UV−vis spectra of the mixed-valence π-cation radicals, on the other hand, display Soret absorptions and α,β bands that show only very small changes in band position compared to the equivalent neutral porphyrin. These mixed-valence bands are broadened relative to the bands displayed by the neutral

(34) Reed, D. *J. Biol. Chem.* **1969**, *244*, 4936.
(35) Parson, W. W.; Cogdell, R. J. *Biochim. Biophys. Acta* **1975**, *416*, 105.
(36) (a) Fajer, J.; Brune, D. C.; Davis, M. S.; Forman, A.; Spaulding, L. D. *Proc. Natl. Acad. Sci. U.S.A.* **1975**, *72*, 4956.
(37) Dutton, P. L.; Kaufmann, K. J.; Chance, B.; Rentzepis, P. M. *FEBS Lett.* **1975**, *60*, 275.
(38) Reimers, J. R.; Hush, N. S. *J. Am. Chem. Soc.* **1995**, *117*, 1302.
(39) Stocker, J. W.; Hug, S.; Boxer, G. S. *Biochim. Biophys. Acta* **1993**, *1144*, 325.
(40) (a) Breton, J.; Nabedryk, E.; Parson, W. W. *Biochemistry* **1992**, *31*, 7503. (b) Parson, W. W.; Nabedryk, E.; Breton, J. In *The Photosynthetic Bacterial Reaction Center II: Structure, Spectroscopy, and Dynamics*; Breton, J., Vermeglio, A., Eds.; Plenum Press: New York, 1992; p 79.

porphyrin. In addition, the mixed-valence π-cation radical spectra show shoulders and additional weaker bands that are similar to those shown by the π-cation radical derivatives. Thus, the observed spectrum of any of the mixed-valence π-cation radicals is close to the sum of the spectra of the two reaction components. The near superposition of the spectral sum of the two reacting components (neutral and π-cation radical) and the mixed-valence π-cation radical products is shown in Figures 3a−d.

It is interesting to compare the spectral changes seen in these new mixed-valence π-cation radicals with related systems. The spectral differences between neutral M(OEP) and the corresponding mixed-valence π-cation radicals are similar to the spectral differences observed between the reduced and photooxidized states of reaction centers.[6e,34,41] This is in distinct contrast to the spectral changes observed between the neutral and singly-oxidized lanthanide, actinide, and early transition metal double-decker reaction center model complexes.[15,42] In the double-decker MP_2 RC model systems, the spectral changes upon oxidation to MP_2^+ are significant broadening and blue shifts in the Soret region and only weak absorptions in the visible region. All of these singly oxidized double-decker derivatives do display a new near-IR band. It is tempting to conclude that the spectral differences in the two model complex systems originate in the structural differences and, in particular, the distinctly different inter-ring orientations known to exist in the solid state. A more complete understanding of the differing spectral changes in the two model systems may come from characterization of their excited state photophysical properties that are currently in progress.

Summary. This study clearly demonstrates the solution stability of partially—but precisely—oxidized metalloporphyrin species that are formally related to the photooxidized special pair of bacterial photosynthesis. The solution reactions of equimolar quantities of neutral and one-electron oxidized metalloporphyrins to yield the novel, mixed-valence, noncovalently-linked, supramolecular products demonstrate the stability that arises from delocalization of a one-electron hole over two porphyrin rings. These mixed-valence π-cation radical complexes display new electronic absorption bands in the near-IR which are not observed in either the neutral M(OEP) or the $[M(OEP^{\bullet})]^+$ π-cation radical derivatives.

Acknowledgment. We thank the National Institutes of Health for support of this research under Grant No. GM-38401. We thank Dr. Robert Warren for helpful discussions on determination of preliminary formation constants.

JA9616950

(41) (a) Vermeglio, A.; Paillotin, G. *Biochim. Biophys. Acta* **1982**, *681*, 32. (b) Clayton, R. K.; Clayton, B. J. *Biochim. Biophys. Acta* **1978**, *501*, 478. (c) Parson, W. W.; Cogdell, R. J. *Biochim. Biophys. Acta* **1975**, *416*, 105.

(42) (a) Buchler, J. W.; De Cian, A.; Elschner, S.; Fischer, J.; Hammerschmitt, P.; Weiss, R. *Chem. Ber.* **1992**, *125*, 107. (b) Buchler, J. W.; Hüttermann, J.; Löffler, J. *Bull. Chem. Soc. Jpn.* **1988**, *61*, 71. (c) Buchler, J. W.; De Cian, A.; Fischer, J.; Kihn-Botulinski, M.; Weiss, R. *Inorg. Chem.* **1988**, *27*, 339.